

FIG. 3. A curve showing the π^+ -meson energy distribution from a 2-inch polyethylene target bombarded by 340-Mev protons. Measurements were made at $0^\circ \pm 7^\circ$ to the proton beam direction. Standard deviations are shown.

In order to compare counter detection of π^+ -meson with plate techniques, the peak spectrum for the reaction $p + p \rightarrow d + \pi^+$ was investigated. This spectrum has been investigated previously by plates.¹ Figure 3 shows the spectrum which was obtained with a 2-inch polyethylene target. The peak occurs at the energy expected from the thick production target which was used. The peak obtained by counters is considerably broader than that obtained by plates because of the greater energy width of the crystal detectors.

Thanks are due Professor C. Richman and co-workers for assistance in all parts of the experiment. We also wish to thank Professor O. Chamberlain for helpful discussions concerning the experiment.

¹ The arrangement was similar to that used by Richman, Skinner, Merritt, and Youtz, Phys. Rev. **80**, 900 (1950).

² Jakobson, Schulz, and Steinberger, Phys. Rev. **81**, 895 (1951).

³ R. F. Mozeley, Phys. Rev. **80**, 493 (1950).

⁴ Brueckner, Serber, and Watson, University California Radiation Laboratory, Phys. Rev. **84**, 258 (1951).

⁵ D. Clark, Phys. Rev. **81**, 313 (1951).

The Positronium Fine Structure*†

RICHARD A. FERRELL

Palmer Physical Laboratory, Princeton University, Princeton, New Jersey

(Received September 27, 1951)

EXPERIMENTAL work now in progress at this laboratory,¹ and elsewhere,² on the fine structure splitting between the 3S and S^1 ground states of positronium make it desirable to study in detail the properties of positronium predicted by the present theory of the electron. The fine structure of the energy levels has been worked out by Pirenne³ and by Berestetski,⁴ apparently independently. With the aim of proceeding to the next higher order (radiative corrections), we have first redone the calculations of these authors, and have found slight errors in both papers. Making

TABLE I. Numerical values of intrinsic positronium fine structure.

	$-\epsilon_{l,j^t}$ and $-\epsilon_{l,j^t}$ for six values of l					
	0	1	2	3	4	5
$-\epsilon_{l,j^s}$	0.5000	0.1667	0.1000	0.0714	0.0555	0.0454
$-\epsilon_{l,l+1}^t$	-0.0833	0.1083	0.0762	0.0585	0.0474	0.0399
$-\epsilon_{l,l}^t$	X	0.2084	0.1083	0.0744	0.0569	0.0462
$-\epsilon_{l,l-1}^t$	X	0.3334	0.1417	0.0904	0.0664	0.0525

the necessary changes in their work is a trivial matter. When this is done, one finds the shifts in energy, ΔE , of the singlet and triplet levels from the nonrelativistic values of $-mc^2\alpha^2/4n^2$ to be

$$\Delta E_{n,l^s} = \frac{11mc^2\alpha^4}{64n^4} + \frac{mc^2\alpha^4}{n^3}\epsilon_{l,j^s}; \quad \Delta E_{n,l,j^t} = \frac{11mc^2\alpha^4}{64n^4} + \frac{mc^2\alpha^4}{n^3}\epsilon_{l,j^t},$$

where ϵ_{l,j^s} and ϵ_{l,j^t} are given by

$$\epsilon_{l,j^s} = -\frac{1}{2} \frac{1}{2l+1}; \quad \epsilon_{l,j^t} = \epsilon_{l,j^s} + \delta_{0l} + \frac{(1-\delta_{0l})}{8(l+\frac{1}{2})} \times \begin{cases} \frac{3l+4}{(l+1)(2l+3)}, & j=l+1 \\ -\frac{1}{l(l+1)}, & j=l \\ -\frac{3l-1}{l(2l-1)}, & j=l-1 \end{cases}$$

(mc^2 is the rest energy of the electron and α the fine structure constant). Since the splittings depend on the principal quantum number, n , only through the factor $mc^2\alpha^4/n^3$, it is possible to study the "intrinsic fine structure" of the quantities ϵ_{l,j^s} and ϵ_{l,j^t} , independent of any particular value of n . ϵ_{l,j^s} and ϵ_{l,j^t} are given numerically and represented schematically in Table I and Fig. 1. One finds the energy levels by adding the common shift, $0.1719/n^3$ and multiplying by $mc^2\alpha^4/n^3 = 11.6 \text{ cm}^{-1}/n^3 = 3.50 \times 10^6 \text{ Mc}/n$, $= 1.45 \times 10^{-3} \text{ ev}/n^3$ (in terms of inverse centimeters, megacycles, or electron volts, respectively). We find the Lamb shift in positronium to be about one-half the corresponding shift in hydrogen

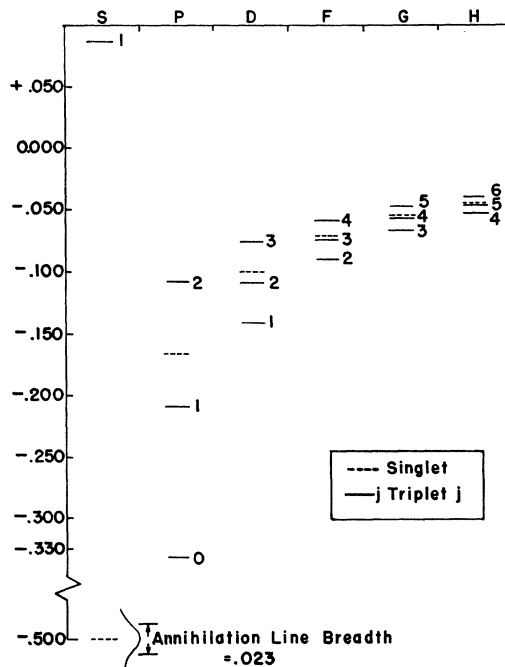


FIG. 1. Intrinsic positronium fine structure. To find energy levels, add $0.1719/n^3$ and multiply by $mc^2\alpha^4/n^3 = 11.6 \text{ cm}^{-1}/n^3 = 3.50 \times 10^6 \text{ Mc}/n = 1.45 \times 10^{-3} \text{ ev}/n^3$.

and to have no prominent effect on the fine structure. It does not reveal itself by splitting a degeneracy, as in the case of the hydrogen atom. Our calculations of the fine structure and its radiative corrections will be published in detail later.

We wish to thank Professor A. S. Wightman for valuable guidance and help in this problem, and the Atomic Energy Commission for support through a Predoctoral Fellowship.

* The work outlined here is part of a Ph.D. thesis to be submitted to Princeton University.

† This work was supported in part by the AEC.

¹ R. H. Dicke and T. A. Pond (private communication).

² M. Deutsch (private communication).

³ J. Pirenne, Arch. sci. phys. et nat. 28, 233 (1946); 29, 121, 207, and 265 (1947). Pirenne omits a term $\pi e^2 \hbar^2 \langle r \rangle / m^2 c^2$ from the orbital interaction, and his spin-orbit energy should be multiplied by 3/2.

⁴ V. B. Berestetski, J. Exptl. Theoret. Phys. (U.S.S.R.) 19, 1130 (1949). See also V. B. Berestetski and L. D. Landau, J. Exptl. Theoret. Phys. (U.S.S.R.) 19, 673 (1949). Berestetski's expressions for the interactions are correct. His evaluation of \bar{V}_4 , however, seems to be in error for $l \neq 0$, for it is too large by a factor of two.

Ionization Potentials and Probabilities Using a Mass Spectrometer

R. E. FOX, W. M. HICKAM, T. KJELDAAS, JR., AND D. J. GROVE
Westinghouse Research Laboratories, East Pittsburgh, Pennsylvania
(Received October 4, 1951)

A METHOD for determining ionization potentials and ionization probability curves has been devised which eliminates the difficulties arising from uncertainties in the energy of the bombarding electrons.¹

A sketch of the ion source is shown in Fig. 1(a). Electrons leaving the filament are accelerated into the ionization enclosure by the potential V_1 . The intermediate electrode 4 is maintained at a negative potential V_R with respect to the filament so as to prevent the low energy electrons in the distribution from entering the ionization chamber. The increase in the ion current observed when the absolute value of V_R is decreased by ΔV_R , keeping V_1 fixed, represents the ion current produced by a beam of electrons monoenergetic within ΔV_R . If V_{4M} is the larger, and V_{4m} the smaller in absolute value of the two corresponding V_4 readings, this then uniquely determines the maximum and minimum energy of the electrons producing the observed difference in ion current [see Fig. 1(b)]. If now the ion current difference is measured and plotted as a function of V_{4M} , keeping V_R constant, this difference will go to zero at the ionization potential. This curve represents the ionization probability as measured with an electron beam monoenergetic within ΔV_R . In a case where the ionization prob-

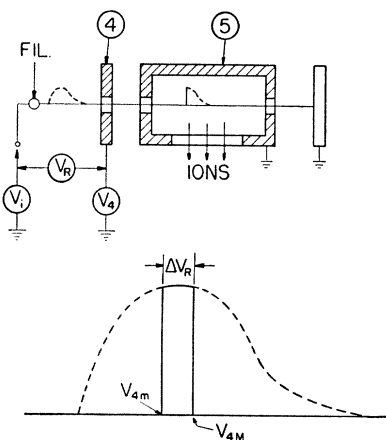


FIG. 1. (a) A sketch of the ion source showing the electrode structure and the voltage references. (b) A distribution in electron energy which is modified by the retarding potential to give the equivalent of a monoenergetic electron beam.

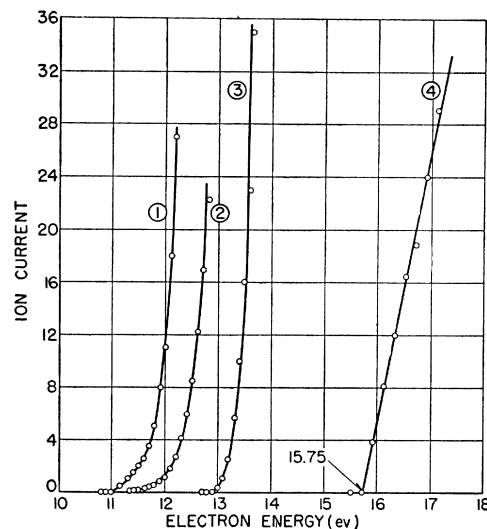


FIG. 2. Ionization probability curves for argon 40^+ . Run (1) taken by conventional method. Run (2) taken by conventional method with 0.1 sensitivity at the amplifier. Run (3) the ion difference curve using a retarding potential on the electrons, but with an ion-draw-out voltage of 3 volts. Run (4) the ion difference curve obtained using both a retardation of the electrons and pulsed fields on ions and electrons.

ability varies linearly with the electron energy, for values of V_{4M} greater than ΔV_R plus the ionization potential, the observed curve should be linear. For values of V_{4M} within ΔV_R above the ionization potential the curve is essentially parabolic, approaching the axis with zero slope at the ionization potential. In the measurements described here, ΔV_R was 0.1 volt and usually no points were taken for V_{4M} within this region. This amounts to extrapolating over the small interval ΔV_R . It may be proved that this will yield a value for the ionization potential too high by $\Delta V_R/2$. To compensate for this, the experimental curves were plotted as a function of the average value of V_4 instead of V_{4M} .

Since the energy scale is determined by the potential between the retarding electrode 4 and the ionization chamber 5 [see Fig. 1(a)] the effect of the contact potentials between the filament and the accelerating electrodes is eliminated. Those contact potentials which can arise between the accelerating electrodes have been reduced or eliminated by gold plating all surfaces.

To obtain ion currents of sufficient magnitude, it is necessary to apply a small electric field across the ionization chamber in a direction normal to the electron beam. In past experiments, this ion-draw-out field created an inhomogeneity and uncertainty in the electron energy. In the present experiments this difficulty has been overcome by giving the electron current and the ion-draw-out voltage a pulsed time dependence such that the electrons reach the ionization chamber only when the draw-out field is zero.

Because magnetic collimation of the electron beam is employed, one might expect that the transverse (spiralling) velocity of the electrons would give rise to a considerable spread in electron energy, which would lead to "tailing" of the ionization probability curve in the region of onset. Experimentally, this "tailing" is not observed, indicating that some mechanism serves to prevent electrons with appreciable transverse energy from reaching the ionization chamber.

Since the electrons are moving very slowly near the retarding plate, space charge effects are quite important in this experiment. By measuring the apparent ionization potential as a function of the electron current, and extrapolating to zero current, a correction term was obtained which was of the order of 0.2 volt for the work reported here. Modifications are underway which should reduce this effect.

Preliminary measurements have been taken on argon (40^+), krypton (84^+), nitrogen (28^+), and carbon monoxide (28^+). In all